Functional MMP-10 is required for efficient tissue repair after experimental hind limb ischemia

Violeta Gomez-Rodriguez,* Josune Orbe,* Esther Martinez-Aguilar,[†] Jose A. Rodriguez,* Leopoldo Fernandez-Alonso,[†] Jens Serneels,[‡,§] Miriam Bobadilla,[¶] Ana Perez-Ruiz,[¶] Maria Collantes,[∥] Massimiliano Mazzone,[‡,§] Jose A. Paramo,*[,1] and Carmen Roncal*[,1]

*Laboratory of Atherothrombosis, Division of Cardiovascular Sciences, and [¶]Cell Therapy Area, Division of Cancer, Center for Applied Medical Research (CIMA), University of Navarra, Pamplona, Spain; [†]Department of Vascular Surgery, Complejo Hopitalario de Navarra, Pamplona, Spain; [‡]Laboratory of Molecular Oncology and Angiogenesis, Vesalius Research Center, VIB, Leuven, Belgium; [§]Laboratory of Molecular Oncology and Angiogenesis, Vesalius Research Center, Department of Oncology, KU Leuven, Leuven, Belgium; and [∥]Small Animal Imaging Research Unit, CIMA and Clínica Universidad de Navarra, Pamplona, Spain

ABSTRACT   We studied the role of matrix metalloproteinase-10 (MMP-10) during skeletal muscle repair after ischemia using a model of femoral artery excision in wild-type (WT) and MMP-10 deficient ($Mmp10^{-/-}$) mice. Functional changes were analyzed by small animal positron emission tomography and tissue morphology by immunohistochemistry. Gene expression and protein analysis were used to study the molecular mechanisms governed by MMP-10 in hypoxia. Early after ischemia, MMP-10 deficiency resulted in delayed tissue reperfusion (10%, $P < 0.01$) and in increased necrosis (2-fold, $P < 0.01$), neutrophil (4-fold, $P < 0.01$), and macrophage (1.5-fold, $P < 0.01$) infiltration. These differences at early time points resulted in delayed myotube regeneration in $Mmp10^{-/-}$ soleus at later stages (regenerating myofibers: 30 ± 9% WT *vs.* 68 ± 10% $Mmp10^{-/-}$, $P < 0.01$). The injection of MMP-10 into $Mmp10^{-/-}$ mice rescued the observed phenotype. A molecular analysis revealed higher levels of *Cxcl1* mRNA (10-fold, $P < 0.05$) and protein (30%) in the ischemic $Mmp10^{-/-}$ muscle resulting from a lack of transcriptional inhibition by MMP-10. This was further confirmed using siRNA against MMP-10 *in vivo*. Our results demonstrate an important role of MMP-10 for proper muscle repair after ischemia, and suggest that chemokine regulation such as *Cxcl1* by MMP-10 is involved in muscle regeneration.—Gomez-Rodriguez, V., Orbe, J., Martinez-Aguilar, E., Rodriguez, J. A., Fernandez-Alonso, L., Serneels, J., Bobadilla, M., Perez-Ruiz, A., Collantes, M., Mazzone, M., Paramo, J. A., Roncal, C. Functional MMP-10 is required for efficient tissue repair after experimental hind limb ischemia. *FASEB J*. 29, 960–972 (2015). www.fasebj.org

Key Words: hypoxia · inflammation · matrix metalloproteinase · regeneration

MATRIX METALLOPROTEINASES (MMPs), a family of zinc-dependent endopeptidases, contribute extensively to tissue remodeling in a variety of normal and disease processes, including ischemic disorders associated with vascular dysfunction, such as peripheral artery disease (1, 2). Peripheral artery disease is a major cause of acute and chronic illness in Europe and North America. It affects about 5% of the elderly population over 55 yr of age, and increases to 15% to 20% in persons aged over 70 yr, presenting equal morbidity and mortality and comparable (or higher) health economic costs as coronary heart disease and ischemic stroke (3). High gelatinolytic activity is necessary for tissue remodeling in response to arterial occlusion in experimental ischemia (4–7); however, to our knowledge, the contribution of other MMPs, such as stromelysins, has not yet been investigated.

MMP-10 (stromelysin 2) is induced in different cell types, such as inflammatory cells, neurons, or endothelial cells (EC), and presents proteolytic activity against a wide range of extracellular proteins such as collagen types III, IV, and V, fibronectin, or gelatin. It seems to have a predominant role in pathologic conditions related to tissue repair and inflammation (8). In fact, MMP-10 is not detected in normal skin but is localized in migrating keratinocytes at the wound edge during wound healing (9), and it is overexpressed in different tumor types associated with cancer cell migration, invasiveness, and growth (10–12). In addition, its expression is detected in EC and macrophages within human atherosclerotic plaques (13). We have shown that circulating levels of MMP-10 correlate with cardiovascular risk factors in apparently healthy subjects (14) and is associated with inflammation and

[1] Correspondence: Laboratory of Atherothrombosis, Division of Cardiovascular Sciences, CIMA, Av. Pio XII, 55. 31008, Pamplona, Navarra, Spain. E-mail: japaramo@unav.es and croncalm@unav.es

thrombin generation (15, 16). A role for MMP-10 in neovascularization has also been proposed, though it is unclear whether its activity is more important at the beginning of the angiogenic process or later on for the stabilization and maintenance of the newly formed capillaries (17–19).

We sought to determine the role of MMP-10 in tissue remodeling upon ischemic injury. Thus, we subjected wild-type (WT) and MMP-10 deficient ($Mmp10^{-/-}$) mice to a model of femoral artery excision and analyzed functional, morphologic, and molecular abnormalities associated with MMP-10 inactivation.

MATERIALS AND METHODS

Hind limb ischemia model

Male WT (C57Bl/6) and MMP-10 deficient mice ($Mmp10^{-/-}$, C57Bl/6J background N8), kindly provided by Dr. W. C. Parks (12-wk-old, $n = 6$ to 10 per genotype per group), were anesthetized with isoflurane (2.5% to 4%, inhaled; IsoVet; Piramal Healthcare, Morpeth, Northumberland, United Kingdom) and underwent surgery under sterile conditions. A longitudinal incision was made in the skin overlying the middle portion of the right hind limb. The nonligated left limb was used as control. The femoral artery and vein were both ligated proximal to the inguinal ligament and right before the bifurcation to the saphenous and popliteal arteries. The artery and vein and all side branches were dissected and excised (20). All animals received an anti-inflammatory agent (ketoprofen, 5 mg/kg s.c.; Ketofarm; Fatro Ibérica, Barcelona, Spain) daily for 3 d and an antibiotic (enrofloxacin, 25 mg/kg, in drinking water; Alsir; Esteve Veterinaria, Barcelona, Spain) for 3 d after surgery.

For the rescue assay, recombinant human MMP-10 (rhMMP-10) was produced in a mammalian cell system, purified, and activated following a previously described procedure (21). Mice were injected through the femoral vein with active rhMMP-10 (2 nmol/L, ≈6.5 μg/kg) or vehicle (50 mM Tris, 10 mM CaCl, 15 mM NaCl, 0.05% Brij 35, pH 7.5) as control right after ligation or 24 h after ischemia.

The research was performed in accordance with the European Community guidelines for ethical animal care and use of laboratory animals (Directive 2010/63/EU), and approved by the Animal Research Ethics Committee of the University of Navarra.

Model of muscle injury by notexin

A model of muscular injury was performed on male WT mice (C57Bl/6) where 10 μl of notexin from *Notechis scutatus scutatus* (10 μg/ml; Latoxan; Valence, Drôme, France) were injected i.m. into the right tibialis anterior muscle (TA), whereas left muscle received PBS. Twenty-four hours after the notexin injection, MMP-10 was silenced by preparing 2 pooled siMMP-10 duplexes (43200844, s69911, and s69910; Ambion; Life Technologies, Austin, TX, USA) in atelocollagen (Koken; Bunkyo-ku, Tokyo, Japan), according to the manufacturer's instructions, and injecting them i.m. into the right damaged TA, whereas control siRNA was administered into the left muscle after 24 h.

Tissue perfusion small animal positron emission tomography (microPET)

Twenty-minute-duration microPET (Philips Mosaic HP Small Animal PET Imager; Philips Electronics) studies were performed 10 min after ^{13}N-ammonia injection as described previously (20). Briefly, mice were anesthetized with 2% isoflurane in 100% O_2 gas for ^{13}N-ammonia injection (75 MBq) in the tail vein and were kept under such conditions during the entire study. PET scans were performed at d 1, 3, 7, 15, and 24 after surgery. For quantitative analysis and further comparisons among subjects, evaluation of perfusion was performed as previously described (20).

Histologic analysis in mice after femoral artery excision

Mice were humanely killed at d 3, 15, and 28 after excision by CO_2 inhalation and perfused with saline. After death, their soleus muscles were dissected. Tissues were fixed overnight in 2% phosphate-buffered paraformaldehyde, dehydrated, and embedded in paraffin. Tissue sections were stained with rat anti-mouse CD31 (Dianova, Hamburg, Germany), rat anti-mouse F4/80 (AbD Serotec, Hercules, CA, USA), rat anti-mouse NIMP-R14 (Abcam, Cambridge, United Kingdom), rabbit anti-mouse chemokine (C-X-C motif) ligand 1 (CXCL1; Acris, San Diego, CA, USA), rabbit anti-human MMP-10 (Acris), and rabbit anti-mouse Laminin (Sigma-Aldrich, St. Louis, MO, USA) antibodies followed by incubation with peroxidase-labeled secondary IgGs (Dako, Glostrup, Hovedstaden, Denmark) and amplification with the proper tyramide signal amplification system (PerkinElmer, Waltham, MA, USA) in the case of F4/80, or with Envision anti-rabbit (Dako) for CD31 antibody. Hematoxylin and eosin (H&E) staining was used to evaluate the necrosis and the regeneration rate. Sirius Red staining was performed in soleus sections to evaluate total collagen deposition. Morphometric analysis was performed using a Nikon Eclipse 80i microscope (Nikon Instruments, Melville, NY, USA) with Cell^D software for collagen and F4/80 analysis and Fiji image analysis software for any other case.

Isolation of peritoneal leukocytes

Twelve-week-old WT and $Mmp10^{-/-}$ mice were humanely killed by CO_2 inhalation and were injected i.p. with 8 ml of ice-cold PBS into the peritoneal cavity using a 26-gauge half-inch needle. After gently massaging the belly, 5 ml of PBS were retrieved from the peritoneal cavity using an 18-gauge half-inch needle. Cells were centrifuged at 1200 rpm at 4°C for 5 min. The resulting pellet was resuspended in red blood cell lysis buffer (Sigma-Aldrich) and stored at −80°C for RNA isolation.

Gene expression analysis

RNA from tissues and cells was extracted using a semiautomated system for the isolation and purification of nucleic acids (ABI Prism 6100; Applied Biosystems, Life Technologies, Foster City, CA, USA) and 1 μg was reverse transcribed with random primers and Moloney murine leukemia virus reverse transcriptase (Invitrogen, Life Technologies, Carlsbad, CA, USA). A total of 200 ng of cDNA were taken for real-time quantitative PCR (qPCR) using TaqMan low-density custom arrays (LDA; Applied Biosystems, Life Technologies) and ABI Prism 7900HT Sequence Detection System (Applied Biosystems, Life Technologies).

Customized 384-well low-density arrays for qPCR amplification were designed using individual primers for genes of interest, chosen and purchased from the assays on demand gene-expression products. A total of 100 μl master mix containing 200 ng cDNA were loaded into each of the 8 ports. The distribution into 48 reaction cavities per port was carried out by 2 short centrifugation steps (1 min 1200 rpm in a swinging bucket rotor, Rotina 35R, Hettich). *β-Actin* was used as housekeeping gene.

qPCR was performed on an ABI Prism 7900HT sequence detector (Applied Biosystems, Life Technologies) using TaqMan gene expression assays on demand for mice (Applied Biosystems, Life Technologies) for *Mmp10* (Mm00444630_m1) and *Cxcl1* (Mm00433859_m1). *β-Actin* (Mm.PT.49.9990212.g, PrimeTime

qPCR gene expression assays; IDT, Leuven, Belgium) was used as housekeeping gene. For human gene expression, *Cxcl1* (Hs. PT.58.39039397, IDT) and *Gapdh* (Hs.PT.39a.22214836, IDT) were used.

Western blot analysis

CXCL1 and MMP-10 proteins were measured by Western blot analysis in WT and $Mmp10^{-/-}$ mice tissues (crural muscles). In brief, tissues were collected, frozen, and ground into powder. Proteins were extracted by adding radioimmunoprecipitation assay buffer (Sigma-Aldrich) plus complete protease inhibitors tablet (Roche, Indianapolis, IN, USA), homogenized with polytron (Kinematika AG PT3000; Littau, Lucerne, Switzerland) and centrifuged (10 min, 13,000 rpm, 4°C). Protein concentration was determined by the Bradford assay (Bio-Rad Laboratories, Munich, Bavaria, Germany). A total of 35 to 60 μg total homogenate was loaded into a gel for SDS-PAGE (4% to 12% Bis-Tris gel; Invitrogen, Life Technologies). Proteins were then transferred to a nitrocellulose membrane (iBLOT transfer stacks; Invitrogen, Life Technologies), blocked with 10% milk in TBST (5 mM Tris, 34.25 mM NaCl, 0.1% Tween 20, pH 7.6), and incubated overnight with a rabbit anti-mouse MMP-10 antibody (Acris) or with a rabbit anti-mouse KC antibody (CXCL1, 15 μg/ml; Fitzgerald, North Acton, MA, USA), followed by 1 h incubation with a peroxidase-conjugated goat anti-rabbit antibody (RT, 1:5000; Dako). For the loading control, the membrane was stripped with a stripping buffer (20 min, 37°C; Thermo Scientific, Rockford, IL, USA) and incubated overnight at 4°C with monoclonal anti-GAPDH or monoclonal anti-β-actin antibody (both from Sigma-Aldrich) followed by 1 h incubation with a horseradish peroxidase–conjugated goat anti-mouse antibody (RT, 1:10,000; Santa Cruz, Santa Cruz, CA, USA). Protein detection was developed by a chemiluminiscent substrate ECL Advance for MMP-10 and KC, and ECL Prime for the housekeeping proteins (Western Blotting Detection Kit; GE Healthcare, Buckinghamshire, United Kingdom). Images were captured with the Odyssey imaging system (Li-Cor Biosciences, Lincoln, NE, USA), and their quantification was performed with Image Studio Lite (Li-Cor Biosciences).

CXCL1 cleavage by MMP-10

Human recombinant CXCL1 (R&D Systems, Minneapolis, MN, USA) was incubated with active rhMMP-10 (5:1 substrate/enzyme molar ratio) for 24 h at 37°C in assay buffer (100 mmol/L NaCl, 5 mmol/L CaCl$_2$, 20 mmol/L Tris-HCl, pH 7.5). Digestion products were analyzed by SDS-PAGE gel electrophoresis and stained with GelCode Blue stain reagent (Pierce, Rockford, IL, USA). MMP activity inhibitor GM6001 (Ryss Laboratory, Union City, CA, USA) was used as negative control (1 μM).

Isolation of mouse lung endothelial cells (EC)

EC were isolated from WT and $Mmp10^{-/-}$ mice lungs by collagenase digestion followed by selection with ICAM-2-coated magnetic beads. In short, mice were humanely killed by CO$_2$ inhalation, and lungs were excised and finely minced before collagenase A (0.1%; Gibco, Grand Island, NY, USA) digestion at 37°C for 1 h under shaking. The digested tissue was homogenized with a 14-gauge syringe and centrifuged at 200g for 5 min. Then the cell pellet was extensively washed and seeded in a 1% gelatin-coated flask. After 4 d in culture, EC were recovered and selected using Dynabeads sheep anti-rat IgG (Invitrogen, Life Technologies) coupled to a rat anti-mouse ICAM-2 antibody (BD Pharmingen, San Jose, CA, USA). EC were cultured in DMEM:F-12 medium supplemented with 20% fetal calf serum, 30 mg/ml endothelial cell growth supplement

(Sigma-Aldrich), 100 mg/ml heparin (Sigma-Aldrich), and 1% penicillin/streptomycin (Gibco).

EC stimulation

When EC reached confluence, they were subjected to serum deprivation for 12 h and then stimulated with 2 nM active rhMMP-10; their RNA was collected 12 h later. The RNA was reverse transcribed and analyzed by qPCR as previously described.

WT EC were serum deprived overnight and then preincubated with actinomycin D (ActD; 0.5 μM, 1 h; Sigma-Aldrich), then stimulated with active rhMMP-10 (2 nM) for an additional 12 h and collected for CXCL1 expression analysis. To study the stability of CXCL1 mRNA after serum starvation, cells were stimulated with rhMMP-10 for 12 h and then treated with ActD for 9 h.

Leukocyte transendothelial migration

A total of 100,000 EC in 100 μl complete medium were plated in the upper chamber of gelatin precoated 3 μm pore size Boyden chambers (Transwell Permeable support; Costar, Sigma-Aldrich), and 600 μl complete medium was poured onto the lower chamber. One day after, cells were starved of serum by replacing complete medium with serum-free medium in both chambers. After 24 h, EC were stimulated with 20 ng/ml of TNF-α (Sigma-Aldrich) in serum-free medium for 2 h. In the meantime, intraperitoneal leukocytes were isolated from WT and $Mmp10^{-/-}$ mice (as explained above), resuspended in RPMI 1640 medium (0.5% bovine serum albumin, 1% penicillin/streptomycin), and stained with 0.2 μM of calcein (Molecular Probes, Life Technologies) for 30 min at 37°C. Then the medium in the lower chamber was replaced by stimulation medium (RPMI 0.5% bovine serum albumin, 1% penicillin/streptomycin, 100 ng/ml MCP-1; Sigma-Aldrich) and the medium of the upper chamber by 150,000 calcein-stained leukocytes in 100 μl of RPMI (0.5% bovine serum albumin, 1% penicillin/streptomycin). Cells were incubated for 2 h at 37°C. Migrated monocytes were detached from the lower chamber by incubation with cold PBS (5 mM EDTA) for 5 min at 4°C. The resulting supernatant was centrifuged at 1500 rpm during 5 min and stained for CD45 (APC anti-mouse CD45; BD Pharmingen, San Jose, CA, USA) for flow cytometry analysis (FACSCalibur; BD Bioscience, San Jose, CA, USA).

Assessment of signaling pathways

HUVEC were isolated from umbilical cords by digestion with collagenase A (Invitrogen) and cultured as described (22). Cells were seeded in multiwell plates and at confluence were arrested overnight. HUVEC were pretreated for 30 min with inhibitors of intracellular signaling pathways at the following concentrations: 10 μM PD98059 (MEK1/2 inhibitor; Sigma-Aldrich), 10 μM SB203580 (p38 MAPK inhibitor; Sigma-Aldrich), 10 μM SP600125 (JNK inhibitor; Sigma-Aldrich), and 1 μM wortmannin (phosphatidylinositol-3 kinase [PIK3] inhibitor; Sigma-Aldrich) before stimulation with active rhMMP10 (2 nM). Twelve hours later, cells were collected for gene expression analysis.

Statistical analysis

Results from *in vivo* and *in vitro* studies are expressed as mean ± SEM. Statistical analysis was performed by the Kruskal-Wallis test followed by the Mann-Whitney U test for comparisons between groups for independent samples. Paired samples were analyzed by Friedman's test, followed by the Wilcoxon test to compare

between 2 related samples. Statistical significance was established as $P < 0.05$. Statistical analysis was performed by SPSS for Windows software, version 15.0 (IBM, Armonk, NY, USA).

RESULTS

MMP-10 expression is up-regulated in skeletal muscle after ischemia

To determine whether ischemia could trigger the expression of MMP-10 in skeletal muscle, WT mice were subjected to total excision of the femoral artery (20) and their crural muscles collected at different time points (**Fig. 1**). *Mmp10* mRNA was barely detectable at baseline and increased drastically within 72 h after femoral artery excision (Fig. 1*A*, $P < 0.05$). This was confirmed by Western blot analysis 3 d after surgery (Fig. 1*B*). At the regenerative phase (d 15 and 28 after excision), *Mmp10* levels were similar to those at baseline (Fig. 1*A*).

We analyzed MMP-10 levels in soleus sections of WT mice at baseline and again at d 3 and 28 after femoral artery ligation. As shown in Fig. 1*C*, at baseline, MMP-10 expression was observed in large and small vessels and as a diffuse cytoplasmatic staining in myocytes. Seventy-two hours after ischemia, the MMP-10 signal increased compared to baseline, mainly localized in EC and the interstitial tissue (Fig. 1*C, D*). Twenty-eight days after ligation, very weak staining was observed for MMP-10 in the soleus (Fig. 1*C*). The observed up-regulation of MMP-10 after femoral artery excision suggests its possible involvement in muscle repair upon ischemia.

Delayed reperfusion and increased necrosis and inflammation in $Mmp10^{-/-}$ mice

After confirming the expression of MMP-10 in skeletal muscle, we performed experiments in WT and $Mmp10^{-/-}$ mice to measure tissue reperfusion (microPET) and the morphologic changes induced by ischemia in the crural muscles. Twenty-four hours after ligation, perfusion was reduced by 70% in the ligated *vs.* nonligated limbs of WT mice (**Fig. 2***A*). Tissue oxygenation increased gradually and was normalized 24 d after ischemia. $Mmp10^{-/-}$ mice presented reduced perfusion 24 and 72 h after excision ($P < 0.05$) and reached WT values by d 7. Our results suggest that MMP-10 inactivation results in delayed tissue reperfusion soon after arterial ischemia.

To examine whether differences observed in tissue reperfusion could influence muscle degeneration, necrosis and inflammation were assessed in soleus sections 72 h after excision. Using H&E staining, we found that $Mmp10^{-/-}$ mice presented increased necrotic area (Fig. 2*B*, $P < 0.001$) compared to WT mice, which was accompanied by increased neutrophil density (NIMP-R14 marker, Fig. 2*C*, $P < 0.001$) and macrophage infiltration (F4/80 marker, Fig. 2*D*, $P < 0.05$).

Because the observed higher leukocyte infiltration is most likely a consequence of increased leukocyte recruitment, we assessed the involvement of MMP-10 in the later by measuring leukocyte transmigration through an endothelial monolayer *in vitro*. As shown in Fig. 2*E*, leukocyte transmigration significantly increased when endothelial cells (EC) were MMP-10 deficient and it was further incremented when both endothelium and leukocytes were negative for MMP-10 ($P < 0.01$).

Finally, we studied whether the exacerbated muscle degeneration observed in MMP-10–deficient mice could be related not only to differences in macrophage numbers but also to their subtypes. Therefore, the number of wound-healing/proangiogenic macrophages (M2-like) was measured in soleus sections 72 h after ischemia by the expression of the MRC1 mannose receptor. No statistical difference in the number of MRC1$^+$F4/80$^+$ cells was detected between the genotypes, although $Mmp10^{-/-}$ mice presented a 50% reduction compared to WT. Overall, our data show an exaggerated inflammatory response after ischemia in absence of MMP-10, manifesting a role for MMP-10 in leukocyte trafficking.

Altered collateralization and neovascularization in $Mmp10^{-/-}$ mice in response to severe ischemia

To address whether reduced perfusion in $Mmp10^{-/-}$ mice early after ischemia was related to a decreased vascularization, we performed immunohistochemistry for α-smooth muscle actin (α-SMA) and CD31 in soleus sections of nonligated (control) and ligated limbs (**Fig. 3***A, B*). WT and $Mmp10^{-/-}$ muscles presented similar arteriole and vessel density at baseline, and a comparable increase 3 and 15 d after ischemia. However, at the final stage of the regenerative phase, the number of α-SMA-positive capillaries and CD31-positive vessels dropped to baseline in WT but remained elevated in $Mmp10^{-/-}$ muscles ($P < 0.05$). These results indicate that MMP-10 function contributes mainly to efficient vessel regression rather than to neovascularization.

MMP-10 does not influence total collagen content in soleus after ischemia

Because deregulated inflammation can be associated with excessive fibrosis and MMPs are essential for the correct remodeling of the extracellular matrix (ECM), we determined whether MMP-10 inactivation could affect total collagen content in ligated limbs (Sirius Red staining). At d 28 after ischemia, the collagen fraction increased similarly in ligated WT (collagen fraction: $9.8 \pm 0.4\%$ control *vs.* $13.6 \pm 0.4\%$ ligated, $n = 10$, $P < 0.05$) and $Mmp10^{-/-}$ soleus (collagen fraction: $10.1 \pm 0.4\%$ control *vs.* $12.9 \pm 0.6\%$ ligated, $n = 10$, $P < 0.05$) compared to the nonligated limbs of the mice, suggesting no role for MMP-10 in overall muscle fibrosis.

Genetic deletion of MMP-10 delays myotube regeneration after ischemia

Ischemia and necrosis trigger skeletal muscle repair, a highly synchronized process that drives well-characterized morphologic changes. Newly formed myofibers present small-caliber and centrally located myonuclei. When the fusion of myogenic cells is completed, myofibers increase in size and myonuclei move to the periphery, making the regenerated muscle morphologically and functionally
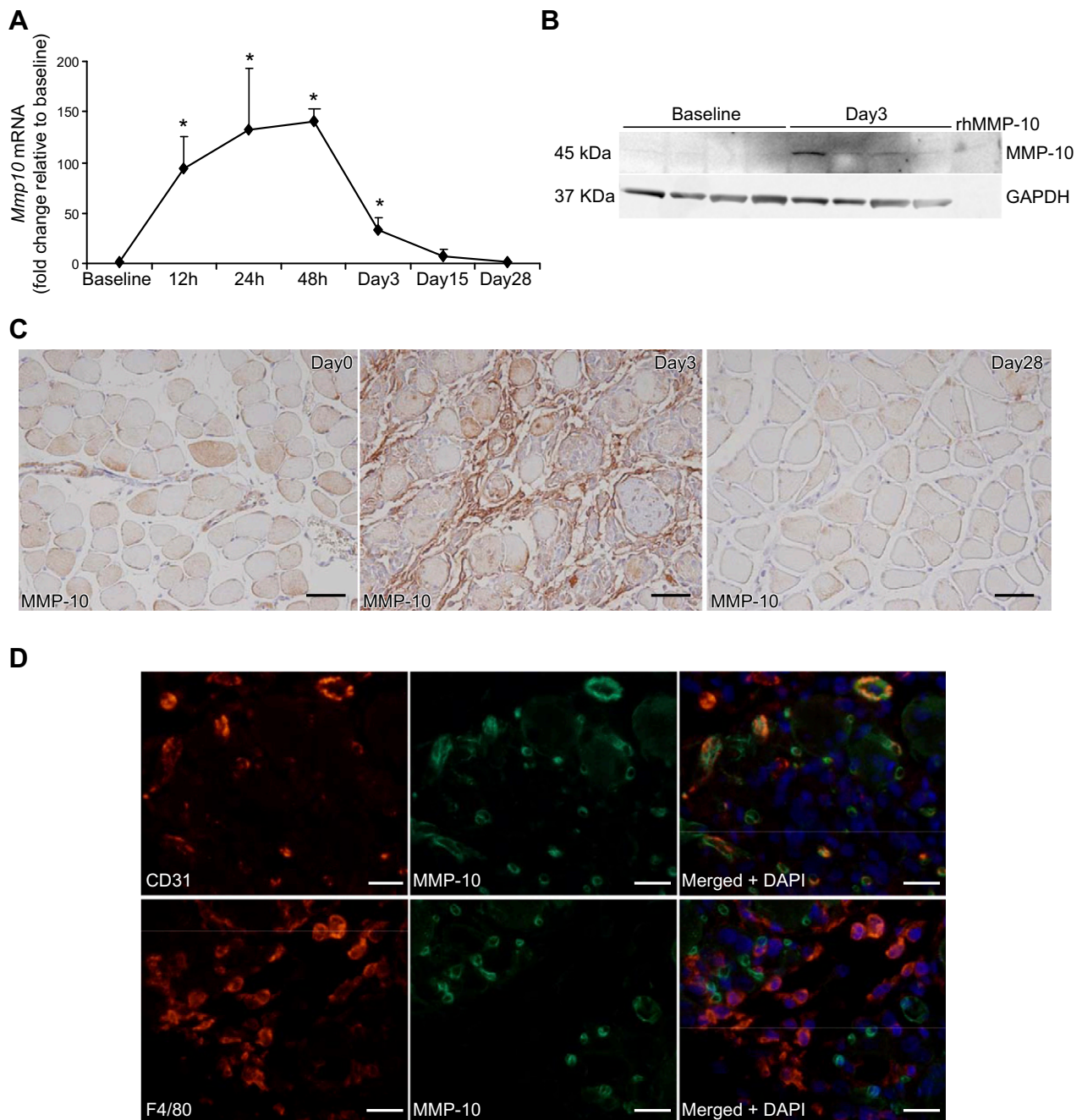
Figure 1. MMP-10 is up-regulated in skeletal muscle after ischemia. *A*) Time course for *Mmp10* mRNA levels in skeletal muscle after femoral artery excision in WT mice. Fold change relative to baseline ($n = 3$ to 5). $*P < 0.05$ *vs.* baseline. *B*) Western blot analysis for MMP-10 and GAPDH (loading control) in WT crural muscles at baseline and d 3 after severe ischemia. Active rhMMP-10 (5 ng) was used as control ($n = 4$ per group). *C*) Immunohistochemistry for MMP-10 in WT soleus at baseline, 3 and 28 d after ischemia. Scale bar, 10 μm. *D*) Double immunofluorecence for MMP-10 and the endothelial marker CD31 (upper line), and the macrophage marker F4/80 (lower line) in WT soleus 72 h after occlusion. Scale bar, 25 μm.

indistinguishable from the undamaged tissue (23). To assess the role of MMP-10 in this process, the myocyte density and the number of centrally nucleated myofibers were measured in soleus sections. The excision of the femoral artery induced a deep regeneration of the skeletal muscle. As a result, WT mice presented an increased number of smaller and centrally nucleated myocytes 15 d after excision compared to controls, and fewer but bigger perinucleated fibers, resembling the morphology of noninjured muscles,

28 d after ischemia (**Fig. 4A–C**). In *Mmp10*$^{-/-}$ soleus muscles, however, myocyte density was lower and cell size bigger than WT mice 15 d after ischemia (Fig. 4*A, B*). At d 28, when the majority of the fibers should be already perinucleated, only 30% of them presented that phenotype in the *Mmp10*$^{-/-}$ mice (Fig. 4*C*), asserting delayed muscle repair. Finally, we determined the fiber-size distribution in laminin-stained soleus sections. At baseline, 70% of the fibers presented sizes between 1000 and 2000 μm^2 in both
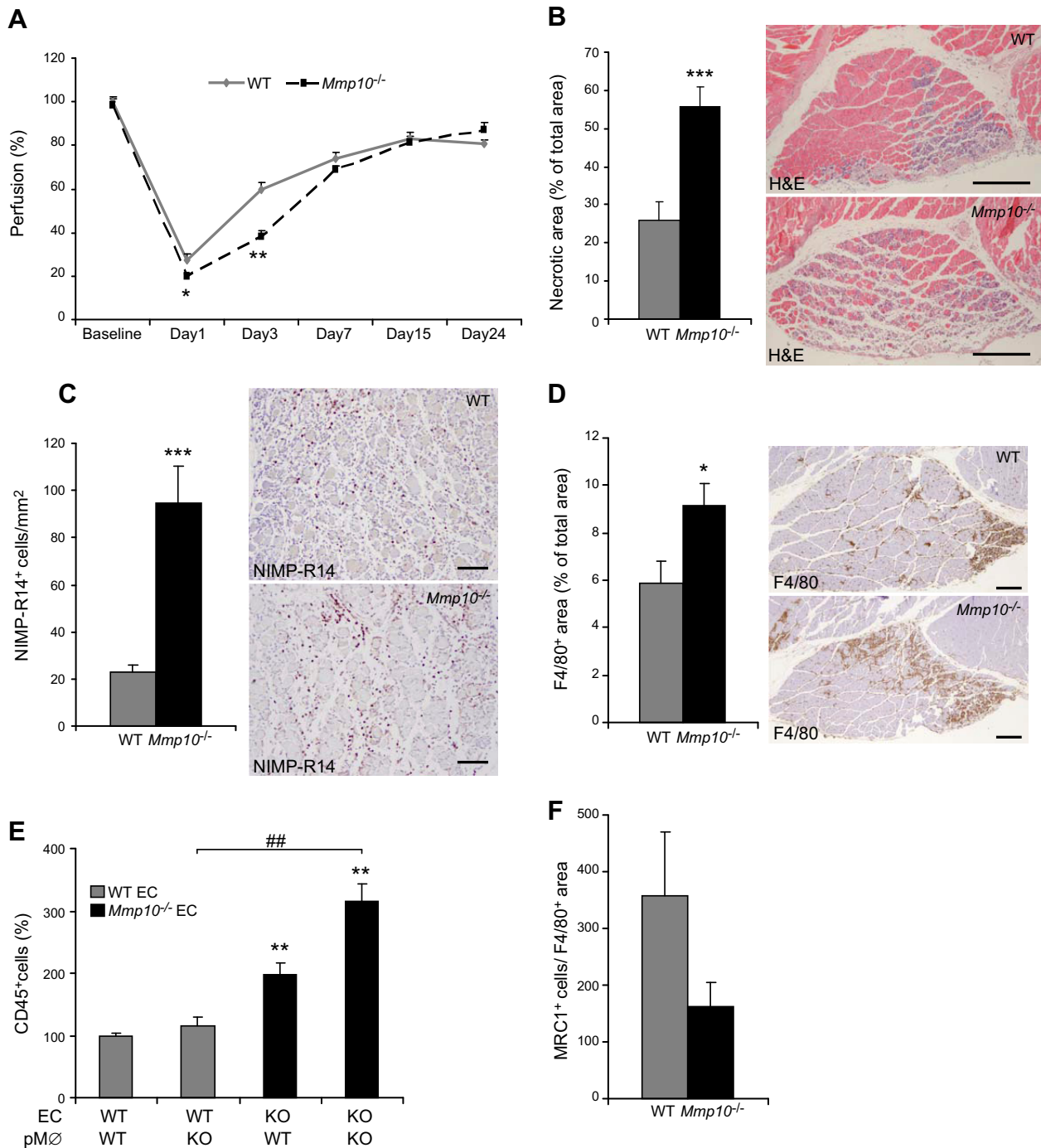
The FASEB Journal · www.fasebj.org

Figure 2. MMP-10 influences tissue perfusion, necrosis and inflammation early after ischemia. *A*) MicroPET analysis shows reduced perfusion in $Mmp10^{-/-}$ mice 1 and 3 d after artery excision ($n = 10$ to 15 per genotype); *$P < 0.05$ and **$P < 0.01$ *vs.* WT. *B*) Necrosis at d 3 after femoral excision ($n = 26$ to 28); ***$P < 0.001$ *vs.* WT. Representative micrographs (H&E staining) of WT and $Mmp10^{-/-}$ soleus 72 h after ligation are shown. Scale bar, 500 μm. *C, D*) Density of NIMP-R14+ (C) and F4/80+ (D) cells at d 3 ($n = 24$ to 27); *$P < 0.05$ and ***$P < 0.001$ *vs.* WT. Representative micrographs of neutrophils (C) and macrophages (D) are shown. Scale bar, 10 μm in (C) and 250 μm in (D). *E*) Genetic deletion of MMP-10 increases leukocyte transendothelial migration *in vitro.* WT and $Mmp10^{-/-}$ (knockout, KO) leukocytes were seeded on top of mouse lung EC monolayers (WT or $Mmp10^{-/-}$) previously stimulated with TNF-α (WT/WT refers to WT EC/ WT pMØ, peritoneal macrophages) (5 independent experiments, $n = 3$ to 6 per experiment); **$P < 0.01$ *vs.* WT/WT. ##$P < 0.01$ *vs.* WT/KO. *F*) Quantification of M2-positive cells (MRC1 marker) in WT and $Mmp10^{-/-}$ soleus ($n = 10^{-7}$).

genotypes (data not shown). As expected, 15 d after ligation, the fiber cross-sectional area was reduced in WT mice compared to baseline conditions (Fig. 4*D*). In contrast, $Mmp10^{-/-}$ mice showed fewer small fibers and increased

frequency of bigger myocytes compared to WT (Fig. 4*D*). At d 28, fiber-size distribution was similar to baseline (70% of the fibers were between 1000 and 2000 μm^2), though the amount of small-size myocytes was slightly increased in
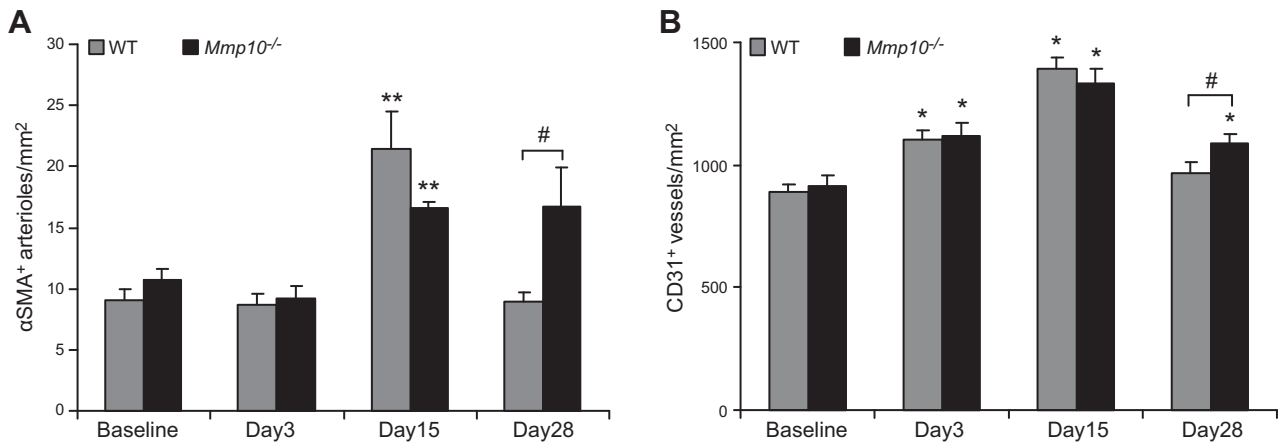
Figure 3. Genetic deficiency of MMP-10 entails delayed vessel regression at the regenerative phase. Morphometric analysis of (*A*) arteriole (α-SMA positive) and (*B*) vessel density (CD31 positive) in soleus sections of WT and $Mmp10^{-/-}$ ligated limbs 3, 15, and 28 d after ligation (*n* = 10). Gray bars correspond to WT mice; black bars correspond to $Mmp10^{-/-}$ mice. *$P < 0.05$ and **$P < 0.01$ *vs.* baseline; #$P < 0.05$ *vs.* WT.

$Mmp10^{-/-}$ soleus tissues (27% $Mmp10^{-/-}$ *vs.* 15% WT, data not shown). These results suggest the requirement of MMP-10 in muscle regeneration after ischemia.

MMP-10 administration to $Mmp10^{-/-}$ mice improves skeletal muscle regeneration

Defective muscle regeneration found after severe ischemia in $Mmp10^{-/-}$ mice prompted us to study whether the systemic administration of rhMMP-10 could restore their healing profile. On the basis of previous studies (21) and data shown in Fig. 1*A*, 2 groups of $Mmp10^{-/-}$ mice were i.v. injected with 6.5 μg/kg of rhMMP-10 or vehicle at different time points. Group 1 was treated with the protein right after ligation to evaluate its effect at the degenerative phase (72 h after ischemia), with vehicle-injected WT mice used as control. Three days after ischemia, $Mmp10^{-/-}$ animals receiving rhMMP-10 presented decreased necrosis ($P < 0.05$) as well as fewer infiltrating neutrophils ($P = 0.07$) and macrophages ($P < 0.05$) compared with untreated $Mmp10^{-/-}$ mice and similar to WT animals (**Fig. 5A–C**).

Group 2 was injected 24 h after ischemia to study the outcome of rhMMP-10 administration at the regenerative phase (28 d after ligation). The percentage of regenerating myofibers at d 28 in rhMMP-10–treated $Mmp10^{-/-}$ mice was much lower than vehicle-injected knockout mice ($P < 0.05$) and similar to that observed for WT animals (Fig. 5*D*). The phenotype of rhMMP-10–treated $Mmp10^{-/-}$ mice was similar to that of WT animals, indicating a direct involvement of MMP-10 in muscle repair.

CXCL1 expression is increased in $Mmp10^{-/-}$ skeletal muscle *in vivo*

To find out the mechanisms and genes mediating MMP-10 function in muscle repair, we isolated lung EC and leukocytes from the peritoneum of WT and $Mmp10^{-/-}$ mice for gene expression analysis by using a low-density array containing a reduced set of genes involved in inflammation and ECM metabolism. Interestingly, $Mmp10^{-/-}$ EC and

leukocytes presented increased expression (~2- and ~3-fold, respectively) of *Cxcl1* (*Groα*) chemokine compared to WT cells (data not shown), which was further confirmed by qPCR (**Fig. 6A, B**). We measured the expression of *Cxcl1* mRNA in the soleus and gastrocnemius crural muscles of WT and $Mmp10^{-/-}$ mice at baseline and different time points after ischemia. As shown in Fig. 6*C*, *Cxcl1* expression was maximal at 12 h and decreased gradually 24 and 48 h after excision in WT mice. In the absence of functional MMP10, *Cxcl1* was strongly up-regulated at 12, 24, and 48 h after ischemia compared to WT conditions ($P < 0.05$, Fig. 6*C*). At later time points, its expression was almost undetectable in both genotypes.

We also performed Western blot analysis for CXCL1 in the crural muscles 12 h after ischemia. As shown in Fig. 6*D*, CXCL1 protein levels were increased (~40%) in $Mmp10^{-/-}$ muscles compared to WT, while it was undetectable at baseline or 28 d after ischemia regardless of genotype (data not shown). In addition, immunofluorescence in control soleus sections showed a similar CXCL1 expression in large vessels and at the periphery of the myofibers in WT and $Mmp10^{-/-}$ mice (data not shown). Three days after ischemia, CXCL1 was localized in myocytes and inflammatory cells and increased by 30% in $Mmp10^{-/-}$ mice compared to WT (Fig. 6*E*, $P < 0.05$). Twenty-eight days after ischemia, the CXCL1 signal was similar to that found at baseline, with no differences between the genotypes (data not shown). Our *in vitro* and *in vivo* results show the overexpression of *Cxcl1* in absence of MMP-10, suggesting the involvement of MMP-10 in CXCL1 regulation in ischemic conditions.

MMP-10 regulates *Cxcl1* expression *in vitro* and *in vivo*

To confirm the participation of MMP-10 in CXCL1 modulation, both proteins were studied in samples from WT mice receiving injections of notexin in the TA to induce muscle injury. After 24 h, MMP-10 expression was reduced in TA muscle using siRNAs. The contralateral muscle was treated with control siRNA (siCtrl). At d 7, TA muscles were collected to measure MMP-10 and CXCL1 expression by Western blot analysis. As shown in **Fig. 7A**, we achieved
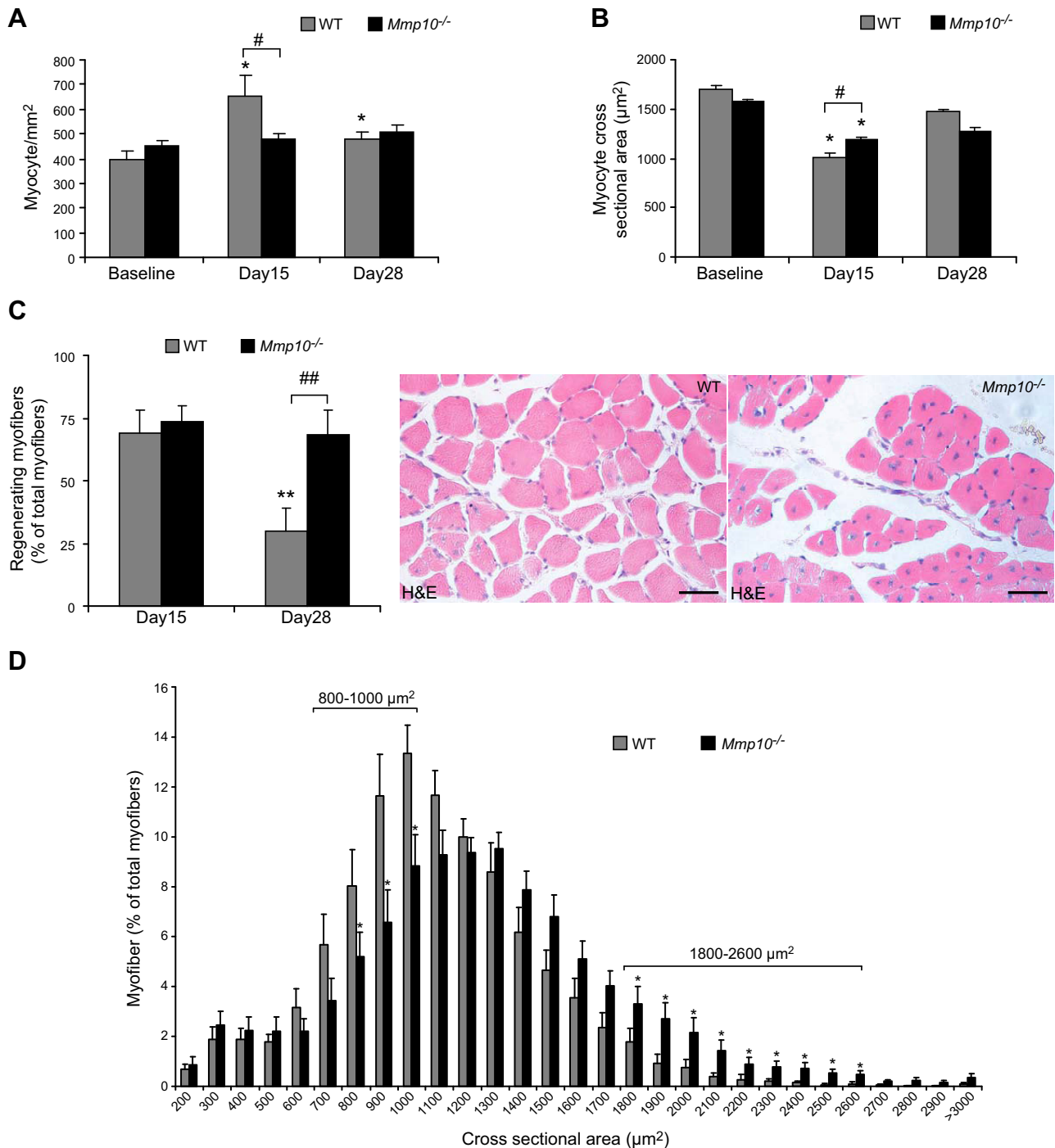
Figure 4. Genetic deletion of MMP-10 delays muscle regeneration after femoral artery occlusion in total excision model. *A)* Myocyte density in soleus sections (H&E staining) at baseline and at d 15 and 28 after femoral artery excision in the ligated limbs ($n = 9$ to 10); *$P < 0.05$ *vs.* baseline; #$P < 0.05$ *vs.* WT. *B)* Myocyte cross-sectional area at different time points; *$P < 0.05$ *vs.* baseline; #$P < 0.05$ *vs.* WT. *C)* Number of regenerating myocytes at d 15 and 28 after femoral artery excision ($n = 9$ to 10); **$P < 0.01$ *vs.* d 15; ##$P < 0.01$ *vs.* WT. Representative micrographs at d 28 are shown. Scale bar, 50 μm. *D)* Fiber size distribution was measured in laminin-stained soleus sections at d 15 after artery excision. *$P < 0.05$ *vs.* WT ($n = 9$ to 10).

a ~50-fold reduction of MMP-10 after gene silencing that was associated with a marked up-regulation (~20-fold) of CXCL1.

The administration of rhMMP-10 to WT mouse lung EC *in vitro* decreased *Cxcl1* mRNA expression 15 h after stimulation (Fig. 7*B*), confirming the regulation of *Cxcl1* expression by MMP-10. The preincubation of WT EC with

ActD, either alone or in combination with rhMMP-10, increased *Cxcl1* expression in WT EC compared to untreated cells (Fig. 7*C*). The addition of ActD after rhMMP-10 stimulation did not further modify the stability of *Cxcl1* mRNA (Fig. 7*D*).

Experiments were performed to determine the signaling pathways involved in CXCL1 regulation by MMP-10.
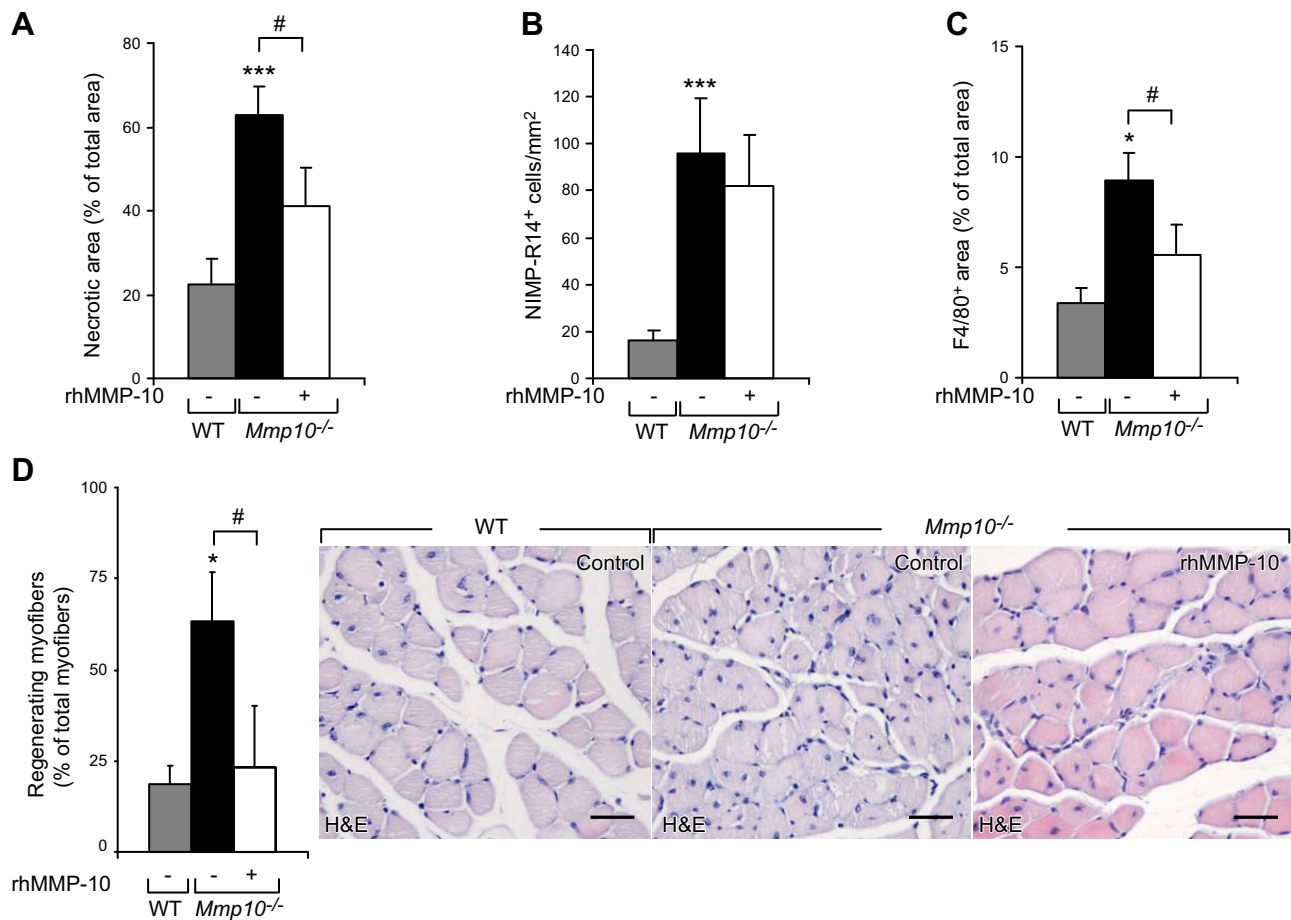
Figure 5. Administration of rhMMP-10 increases muscle recovery in $Mmp10^{-/-}$ mice. *A–C)* Percentage of necrotic area (*A*) and neutrophil (*B*) and macrophage (*C*) infiltration in soleus sections of rhMMP-10-injected animals (group 1) 3 d after femoral artery ligation. Vehicle-injected WT (gray bar), $Mmp10^{-/-}$ (black bar), and rhMMP-10-injected $Mmp10^{-/-}$ mice (white bar); *$P < 0.05$ and ***$P < 0.001$ *vs.* vehicle-injected WT mice ($n = 12$ to 15); #$P < 0.05$ *vs.* vehicle-injected $Mmp10^{-/-}$ mice. *D*) Number of regenerating myocytes in rhMMP-10-treated $Mmp10^{-/-}$ mice 28 d after occlusion (group 2); *$P < 0.05$ *vs.* vehicle-injected WT mice. #$P < 0.05$ *vs.* vehicle injected $Mmp10^{-/-}$ mice ($n = 5$). Representative micrographs show increased number of centrally nucleated cells in $Mmp10^{-/-}$ mice (middle) compared to WT (left) and rhMMP-10-treated null mice (right). Scale bar, 50 μm.

HUVEC were preincubated with inhibitors for MEK1/2 (PD98059), JNK (SP600125), p38MAPK (SB203580), and PIK3 (wortmannin), and then stimulated with rhMMP-10. *Cxcl1* expression was decreased by 50% in rhMMP-10 stimulated cells compared to control (Fig. 7*E*). The pretreatment with the inhibitors PD98059, SP600125, and SB203580 decreased the expression of *Cxcl1* by 30, 46, and 70% respectively, while wortmannin greatly increased its expression. The inhibitory effect (~50%) of rhMMP-10 on CXCL1 expression could not be abrogated by any of the drugs we used, suggesting no involvement of MEK1/2, JNK, p38 MAPK, and PIK3 in the regulation of *Cxcl1* mRNA by MMP-10.

Because MMP-mediated proteolysis can affect the biologic functions of chemokines, we analyzed whether MMP-10 could modify CXCL1 activity by proteolytic cleavage. Thus, recombinant human CXCL1 (rhCXCL1) was incubated for 24 h with active rhMMP-10 and the resulting products analyzed by SDS-PAGE. As shown in Fig. 7*F*, no proteolytic modification of rhCXCL1 was observed in our experimental conditions. Our results show a transcriptional regulation of *Cxcl1* by MMP-10,

although the exact mechanism has to be further determined in future studies.

DISCUSSION

We report that MMP-10 is required for tissue repair after severe hind limb ischemia. Early after ligation, the absence of functional MMP-10 is associated with increased necrosis and with neutrophil and macrophage infiltration that later results in delayed muscle regeneration.

The initial stage of muscle repair is characterized by necrosis of the damaged tissue and activation of the inflammatory response (degeneration) (24). Previous studies showed that the genetic deletion of MMP-2 and MMP-9 reduces macrophage infiltration to the injured tissue in hind limb ischemia (6, 7). However, in our injury model, we found that MMP-10 inactivation increases necrosis and inflammatory cell infiltration. Our results are consistent with previous *in vivo* studies showing augmented inflammation in models of lung infection (8) and muscular dystrophy (25) in $Mmp10^{-/-}$ mice, supporting a role for
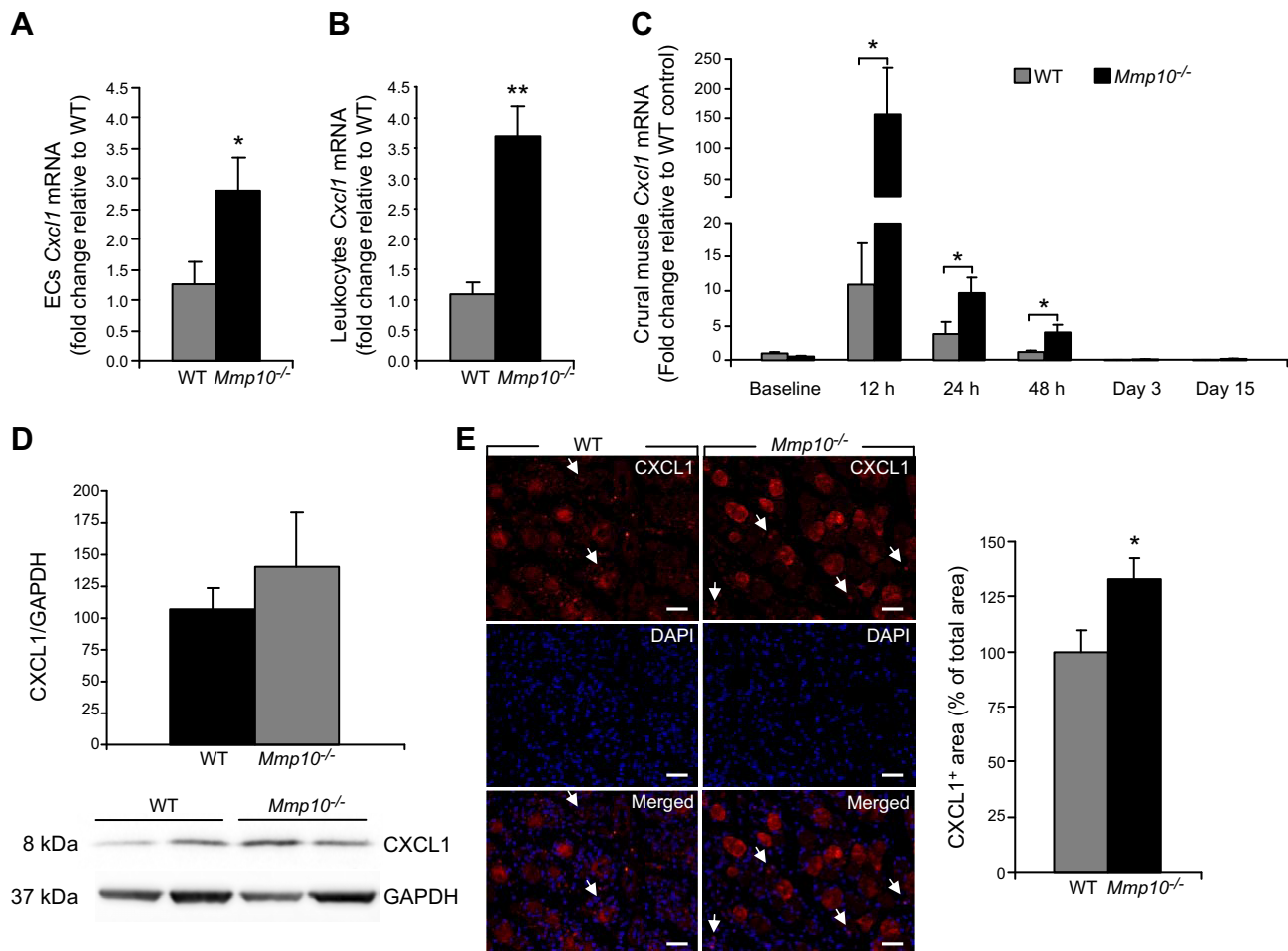
Figure 6. CXCL1 expression is increased in the absence of functional MMP-10 *in vitro* and *in vivo*. *A, B*) *Cxcl1* (*Groα*) expression in $Mmp10^{-/-}$ mouse lung EC (*A*) and leukocytes (*B*) *in vitro* ($n = 5$ to 6); *$P < 0.05$ and **$P < 0.01$ *vs.* WT. *C*) *Cxcl1* mRNA levels in WT and $Mmp10^{-/-}$ skeletal muscle after femoral artery excision ($n = 4$ to 5); *$P < 0.05$ *vs.* WT. *D*) Western blot analysis for CXCL1 in the crural muscles 12 h after occlusion. GAPDH was used as loading control ($n = 4$). *E*) Immunofluorescence for CXCL1 in soleus sections 72 h after ischemia and its quantification; *$P < 0.05$ *vs.* WT ($n = 9$ to 10). Scale bar, 50 μm. Arrowheads indicate leukocytes.

MMP-10 in inflammatory cell trafficking. Phenotypic improvement of $Mmp10^{-/-}$ mice in terms of necrosis and inflammation after systemic rhMMP-10 administration further confirms the direct role of this protease in this initial phase of muscle repair, characterized by inflammation and degeneration. Even though inflammation is essential to activate the molecular pathways responsible for muscle repair, in excess, it might promote tissue deterioration. Likewise, neutrophils, which are the first to infiltrate into the damaged area to elicit the early phagocytic response and to promote macrophage recruitment, can increase tissue deterioration by the release of cytolytic and cytotoxic molecules (26). Macrophages are necessary for tissue regeneration by scavenging apoptotic cells and debris; they produce a vast array of signals involved in matrix remodeling and neovessel formation, but they are also a source of free radicals (26). It should also be considered the activation state of the macrophages, as the proper switch from M1 (proinflammatory) to M2 (anti-inflammatory) is essential for appropriate wound healing (27). *In vivo,* we found decreased number of anti-inflammatory M2 macrophages in $Mmp10^{-/-}$ muscles

that could be partially responsible of the delayed muscle regeneration at later stages compared to WT mice. Whether this delayed polarization toward M2 is directly mediated by the absence of MMP-10 or is a consequence of the sustained inflammatory response observed upon the genetic deletion of MMP-10 will need to be further studied.

We had expected that reduced reperfusion observed in $Mmp10^{-/-}$ mice early after femoral artery ligation would be the result of decreased collateralization at baseline, as has been reported for the TA muscle (25). However, our results show no differences in the collateralization profile between the genotypes in the soleus. Additional studies addressing whether the differences in vascularization between the TA and the soleus muscle are due to the distinct fiber types/metabolic demands of the different muscles will be important to understand the basis for the discrepancy between these studies. Ischemia triggers the activation of arteriogenesis and angiogenesis to restore blood flow. MMPs contribute to these processes by degrading ECM components and by promoting the release of different growth factors (28), thus facilitating smooth muscle cell and EC migration and proliferation. We describe a similar
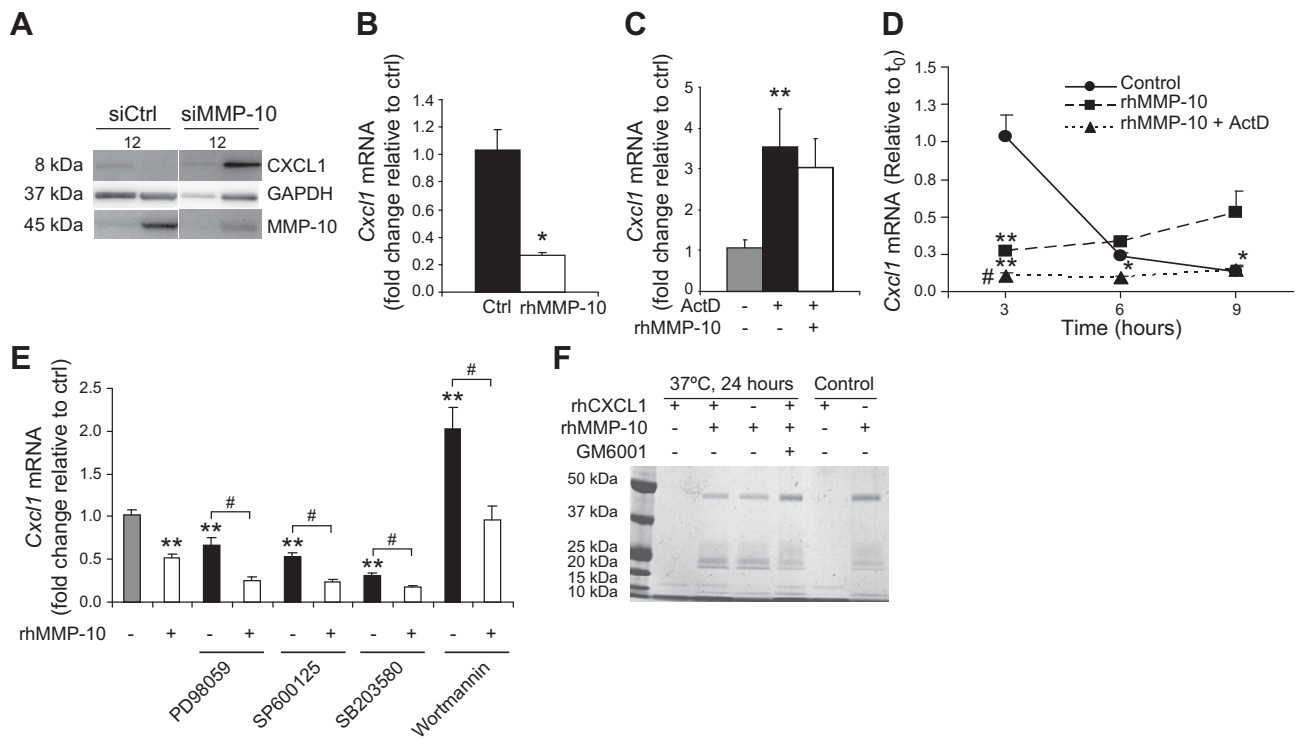
Figure 7. CXCL1 expression is increased in absence of functional MMP-10 *in vivo* and *in vitro*. *A*) Western blot analysis for CXCL1 in siCtrl (left) and siMMP-10 (right) treated TA muscles after notexin administration ($n = 2$ per condition). *B*) *Cxcl1* mRNA expression in rhMMP-10-treated WT EC 15 h after stimulation ($n = 3$ conditions/experiment/2 independent experiments); *$P <$ 0.05 *vs.* vehicle. *C*) Preincubation of WT EC with ActD (1 h, 0.5 μM) increased *Cxcl1* mRNA levels and was not reverted by the posterior addition of rhMMP-10 (12 h, 2 nM) **$P < 0.01$ *vs.* control ($n = 6$). *D*) WT EC were stimulated with rhMMP-10 for 12 h and then treated with ActD for an additional 9 h. Results were plotted as a function of time (relative to time 0). rhMMP-10 reduced *Cxcl1* expression compared to control conditions and remained steady during the experiment; **$P < 0.01$ *vs.* control, #$P < 0.01$ *vs.* rhMMP-10 ($n = 6$). *E*) effect of signaling pathway inhibitors on *Cxcl1* mRNA expression in HUVEC upon rhMMP-10 stimulation ($n = 3$ conditions/experiment/4 independent experiments); **$P < 0.01$ *vs.* control; #$P < 0.01$ *vs.* inhibitor. *F*) SDS-PAGE for recombinant human CXCL1 (rhCXCL1, 15 kDa) after incubation with active rhMMP-10 (45 kDa). No proteolytical cleavage of CXCL1 was observed when incubating with rhMMP-10 for 24 h at 37°C (lines 1 to 4, from left to right). GM6001 was used to inhibit MMP activity (line 4). Lines 5 and 6 are untreated CXCL1 and rhMMP-10, respectively.

arteriogenic and angiogenic response to hypoxia in WT and *Mmp10*$^{-/-}$ mice. At the end of the tissue repair process, when muscle perfusion is restored and regeneration is about to be completed, collateral and capillary density return to baseline conditions in WT mice. *Mmp10*$^{-/-}$ animals, however, present sustained arteriole and capillary density at this time point, suggesting that MMP-10 could be necessary for the process of vessel regression. Other studies have shown that the overexpression of MMP-10 induces capillary tube collapse *in vitro* (19) and vascular rupture *in vivo* (18), supporting the involvement of MMP-10 in vessel relapse rather than in vessel growth.

The inflammatory/damage signals produced in response to tissue injury trigger the activation of satellite cells to proliferate, differentiate, and fuse, leading to new myofiber formation (23, 24, 29). Various experimental models of muscle injury demonstrate the importance of a regulated MMP activity in skeletal muscle repair. MMP-1 and MMP-10 have been shown to improve muscle recovery in different models of tissue injury (25, 30), while muscle repair is only achieved when MMP-9 is inhibited (31). Our study corroborates the requirement of MMP-10 in muscle regeneration after ischemia because delayed myotube differentiation in absence of MMP-10 can be restored

back to WT levels by rhMMP-10 administration. Whether this could be the result of inappropriate satellite cell activation/migration due to impaired degradation of the components of the basal lamina by MMP-10 (25) or by missing signals that limit the damaged tissue to efficiently activate the regenerative program remains an open question.

To study the molecular mechanisms governed by MMP-10 in ischemia, we conducted gene expression analysis and found the up-regulation of the gene encoding for the chemokine *Cxcl1* (*Groα*) in the absence of MMP-10. Our results were confirmed *in vivo* in a model of skeletal muscle damage by toxin injection and, *in vitro,* the addition of MMP-10 decreased *Cxcl1* expression in cell culture. CXCL1 is a member of the CXC chemokine family that has been traditionally related to neutrophil, T lymphocyte, and macrophage chemotaxis (32), cell types essential in the inflammatory response required after injury. Besides its proinflammatory role, a recent study reports that CXCL1 is expressed in murine muscle cells early during *in vitro* myogenesis and is repressed when differentiation is over (33). Other member of this family and its receptor, CXCL12 (SDF1α)/CXCR4, regulate the migration of proliferating and terminally differentiated muscle cells *in*

vitro and in vivo (33, 34). Moreover, the SDF1α/CXCR4 system has been involved in muscle repair after toxin-induced damaged in a MMP-10–dependent mechanism (25). Our study and the studies of others support a role of chemokines in muscle repair after injury and argue toward a strong regulation, either at the RNA or protein level, of chemokines by MMPs. The ability of MMP-10 to modulate chemokines belonging to the same family but with different activities, such as SDF1α, more related to stem cell mobilization, homing, and activation, and CXCL1, mainly associated with inflammatory cell recruitment, further supports the need of MMP-10 at the different stages of muscle repair. We conducted different *in vitro* experiments to determine how MMP-10 could regulate CXCL1. Our results show a transcriptional regulation of *Cxcl1* by MMP-10, although the exact mechanism has to be further determined in future studies. TNF-α, VEGF, or IL-1 have been reported to modulate CXCL1 expression and release through the activation of MAPK (35–37). Thus, we performed experiments to determine if that was also the case for MMP-10. Our results showed no effect of those inhibitors on preventing *Cxcl1* repression by MMP-10, suggesting the involvement of other molecular pathways in MMP-10-mediated *Cxcl1* regulation. We also explored whether MMP-10 could modulate the activity of CXCL1 by proteolytical processing, as described for other MMPs and chemokines (38–41), but no evidence for cleavage involvement was found. Thus, we propose that the transcriptional up-regulation of CXCL1 in crural muscles of $Mmp10^{-/-}$ mice after ligation would represent one, but not the only, mechanism involved in the reported phenotype by enhancing inflammation at the degenerative phase and delaying myogenesis at the reparative stage. Our study reports the involvement of MMP-10 in CXCL1 regulation, but it does not rule out its possible role on the modulation of other chemokines and cytokines. Broader studies, such as those that use microarrays, analyzing the expression of other members of the chemokine and cytokine families in absence of functional MMP-10 would be helpful to understand how MMP-10 contributes to tissue remodeling.

Despite the high degree of homology, each MMP family member presents different regulation, substrate affinities, and time- and space-dependent activation. Therefore, it is not surprising to find distinct or even opposite activities among MMPs in similar experimental conditions or human pathologies. We report here that $Mmp10^{-/-}$ mice present increased inflammatory cell infiltration and normal neovascularization after injury, while previous studies described reduced macrophage infiltration and neovascularization in MMP-2– and MMP-9–deficient animals (4–7). Moreover, at the regenerative phase, the absence of MMP-10 results in delayed skeletal muscle repair after severe ischemia, although no differences in muscle morphology were observed at baseline, as described for MT1-MMP (42). In addition, we did not find differences in muscle fibrosis in absence of functional MMP-10, whereas MMP-1, MMP-2, or MMP-9 are involved in ECM remodeling (43), suggesting the need of examining individual MMPs to understand their biology and function. The latter will encourage the design of drugs targeting specific MMPs. In particular, the manipulation of MMP-10 might provide a new approach for protection against ischemia in human pathologies.

Skeletal muscle repair after injury is a highly synchronized process that comprises 2 interdependent processes, inflammation and myogenesis, with the proper activation and resolution of the former being essential for the correct initiation of the latter. We propose that functional MMP-10 is required for skeletal muscle repair after ischemia by influencing the inflammatory response during the degenerative phase, which later will modulate myocyte differentiation during the regenerative phase. The molecular mechanisms underlying this process could be at least partially explained by the regulation of CXCL1. [Fj]

REFERENCES

1. Busti, C., Falcinelli, E., Momi, S., and Gresele, P. (2010) Matrix metalloproteinases and peripheral arterial disease. *Intern. Emerg. Med.* **5**, 13–25

2. Rodriguez, J. A., Orbe, J., Martinez de Lizarrondo, S., Calvayrac, O., Rodriguez, C., Martinez-Gonzalez, J., and Paramo, J. A. (2008) Metalloproteinases and atherothrombosis: MMP-10 mediates vascular remodeling promoted by inflammatory stimuli. *Front. Biosci.* **13**, 2916–2921

3. Hirsch, A. T., Allison, M. A., Gomes, A. S., Corriere, M. A., Duval, S., Ershow, A. G., Hiatt, W. R., Karas, R. H., Lovell, M. B., McDermott, M. M., Mendes, D. M., Nussmeier, N. A., and Treat-Jacobson, D.; American Heart Association Council on Peripheral Vascular Disease; Council on Cardiovascular Nursing; Council on Cardiovascular Radiology and Intervention; Council on Cardiovascular Surgery and Anesthesia; Council on Clinical Cardiology; Council on Epidemiology and Prevention. (2012) A call to action: women and peripheral artery disease: a scientific statement from the American Heart Association. *Circulation* **125**, 1449–1472

4. Muhs, B. E., Gagne, P., Plitas, G., Shaw, J. P., and Shamamian, P. (2004) Experimental hindlimb ischemia leads to neutrophil-mediated increases in gastrocnemius MMP-2 and -9 activity: a potential mechanism for ischemia induced MMP activation. *J. Surg. Res.* **117**, 249–254

5. Frisdal, E., Teiger, E., Lefaucheur, J. P., Adnot, S., Planus, E., Lafuma, C., and D'ortho, M. P. (2000) Increased expression of gelatinases and alteration of basement membrane in rat soleus muscle following femoral artery ligation. *Neuropathol. Appl. Neurobiol.* **26**, 11–21

6. Cheng, X. W., Kuzuya, M., Nakamura, K., Maeda, K., Tsuzuki, M., Kim, W., Sasaki, T., Liu, Z., Inoue, N., Kondo, T., Jin, H., Numaguchi, Y., Okumura, K., Yokota, M., Iguchi, A., and Murohara, T. (2007) Mechanisms underlying the impairment of ischemia-induced neovascularization in matrix metalloproteinase 2–deficient mice. *Circ. Res.* **100**, 904–913

7. Johnson, C., Sung, H. J., Lessner, S. M., Fini, M. E., and Galis, Z. S. (2004) Matrix metalloproteinase-9 is required for adequate angiogenic revascularization of ischemic tissues: potential role in capillary branching. *Circ. Res.* **94**, 262–268

8. Kassim, S. Y., Gharib, S. A., Mecham, B. H., Birkland, T. P., Parks, W. C., and McGuire, J. K. (2007) Individual matrix metalloproteinases control distinct transcriptional responses in airway epithelial cells infected with *Pseudomonas aeruginosa*. *Infect. Immun.* **75**, 5640–5650

9. Wilkins-Port, C. E., and Higgins, P. J. (2007) Regulation of extracellular matrix remodeling following transforming growth

factor-beta1/epidermal growth factor-stimulated epithelial–mesenchymal transition in human premalignant keratinocytes. *Cells Tissues Organs (Print)* **185**, 116–122

10. Gill, J. H., Kirwan, I. G., Seargent, J. M., Martin, S. W., Tijani, S., Anikin, V. A., Mearns, A. J., Bibby, M. C., Anthoney, A., and Loadman, P. M. (2004) MMP-10 is overexpressed, proteolytically active, and a potential target for therapeutic intervention in human lung carcinomas. *Neoplasia* **6**, 777–785

11. Martinez, C., Bhattacharya, S., Freeman, T., Churchman, M., and Ilyas, M. (2005) Expression profiling of murine intestinal adenomas reveals early deregulation of multiple matrix metalloproteinase (Mmp) genes. *J. Pathol.* **206**, 100–110

12. Van Themsche, C., Alain, T., Kossakowska, A. E., Urbanski, S., Potworowski, E. F., and St-Pierre, Y. (2004) Stromelysin-2 (matrix metalloproteinase 10) is inducible in lymphoma cells and accelerates the growth of lymphoid tumors in vivo. *J. Immunol.* **173**, 3605–3611

13. Montero, I., Orbe, J., Varo, N., Beloqui, O., Monreal, J. I., Rodríguez, J. A., Díez, J., Libby, P., and Páramo, J. A. (2006) C-reactive protein induces matrix metalloproteinase-1 and -10 in human endothelial cells: implications for clinical and subclinical atherosclerosis. *J. Am. Coll. Cardiol.* **47**, 1369–1378

14. Orbe, J., Montero, I., Rodríguez, J. A., Beloqui, O., Roncal, C., and Páramo, J. A. (2007) Independent association of matrix metalloproteinase-10, cardiovascular risk factors and subclinical atherosclerosis. *J. Thromb. Haemost.* **5**, 91–97

15. Lorente, L., Martín, M. M., Labarta, L., Díaz, C., Solé-Violán, J., Blanquer, J., Orbe, J., Rodríguez, J. A., Jiménez, A., Borreguero-León, J. M., Belmonte, F., Medina, J. C., Lliminaña, M. C., Ferrer-Agüero, J. M., Ferreres, J., Mora, M. L., Lubillo, S., Sánchez, M., Barrios, Y., Sierra, A., and Páramo, J. A. (2009) Matrix metalloproteinase-9, -10, and tissue inhibitor of matrix metalloproteinases-1 blood levels as biomarkers of severity and mortality in sepsis. *Crit. Care* **13**, R158

16. Coll, B., Rodríguez, J. A., Craver, L., Orbe, J., Martínez-Alonso, M., Ortiz, A., Díez, J., Beloqui, O., Borras, M., Valdivielso, J. M., Fernández, E., and Páramo, J. A. (2010) Serum levels of matrix metalloproteinase-10 are associated with the severity of atherosclerosis in patients with chronic kidney disease. *Kidney Int.* **78**, 1275–1280

17. Burbridge, M. F., Cogé, F., Galizzi, J. P., Boutin, J. A., West, D. C., and Tucker, G. C. (2002) The role of the matrix metalloproteinases during in vitro vessel formation. *Angiogenesis* **5**, 215–226

18. Chang, S., Young, B. D., Li, S., Qi, X., Richardson, J. A., and Olson, E. N. (2006) Histone deacetylase 7 maintains vascular integrity by repressing matrix metalloproteinase 10. *Cell* **126**, 321–334

19. Saunders, W. B., Bayless, K. J., and Davis, G. E. (2005) MMP-1 activation by serine proteases and MMP-10 induces human capillary tubular network collapse and regression in 3D collagen matrices. *J. Cell Sci.* **118**, 2325–2340

20. Peñuelas, I., Aranguren, X. L., Abizanda, G., Martí-Climent, J. M., Uriz, M., Ecay, M., Collantes, M., Quincoces, G., Richter, J. A., and Prósper, F. (2007) (13)N-ammonia PET as a measurement of hindlimb perfusion in a mouse model of peripheral artery occlusive disease. *J. Nucl. Med.* **48**, 1216–1223

21. Orbe, J., Barrenetxe, J., Rodriguez, J. A., Vivien, D., Orset, C., Parks, W. C., Birkland, T. P., Serrano, R., Purroy, A., Martinez de Lizarrondo, S., Angles-Cano, E., and Páramo, J. A. (2011) Matrix metalloproteinase-10 effectively reduces infarct size in experimental stroke by enhancing fibrinolysis via a thrombin-activatable fibrinolysis inhibitor-mediated mechanism. *Circulation* **124**, 2909–2919

22. Orbe, J., Chordá, C., Montes, R., and Páramo, J. A. (1999) Changes in the fibrinolytic components of cultured human umbilical vein endothelial cells induced by endotoxin, tumor necrosis factor-alpha and interleukin-1alpha. *Haematologica* **84**, 306–311

23. Karalaki, M., Fili, S., Philippou, A., and Koutsilieris, M. (2009) Muscle regeneration: cellular and molecular events. *In Vivo* **23**, 779–796

24. Chargé, S. B., and Rudnicki, M. A. (2004) Cellular and molecular regulation of muscle regeneration. *Physiol. Rev.* **84**, 209–238

25. Bobadilla, M., Sainz, N., Abizanda, G., Orbe, J., Rodriguez, J. A., Paramo, J. A., Prosper, F., and Perez-Ruiz, A. (2014) The

26. Tidball, J. G., and Villalta, S. A. (2010) Regulatory interactions between muscle and the immune system during muscle regeneration. *Am. J. Physiol. Regul. Integr. Comp. Physiol.* **298**, R1173–R1187

27. Kharraz, Y., Guerra, J., Mann, C. J., Serrano, A. L., and Muñoz-Cánoves, P. (2013) Macrophage plasticity and the role of inflammation in skeletal muscle repair. *Mediators Inflamm.* **2013**, 491497

28. Davis, G. E., and Senger, D. R. (2005) Endothelial extracellular matrix: biosynthesis, remodeling, and functions during vascular morphogenesis and neovessel stabilization. *Circ. Res.* **97**, 1093–1107

29. Chen, X., and Li, Y. (2009) Role of matrix metalloproteinases in skeletal muscle: migration, differentiation, regeneration and fibrosis. *Cell Adhes. Migr.* **3**, 337–341

30. Wang, W., Pan, H., Murray, K., Jefferson, B. S., and Li, Y. (2009) Matrix metalloproteinase-1 promotes muscle cell migration and differentiation. *Am. J. Pathol.* **174**, 541–549

31. Zimowska, M., Olszynski, K. H., Swierczynska, M., Streminska, W., and Ciemerych, M. A. (2012) Decrease of MMP-9 activity improves soleus muscle regeneration. *Tissue Eng. Part A* **18**, 1183–1192

32. Bechara, C., Chai, H., Lin, P. H., Yao, Q., and Chen, C. (2007) Growth related oncogene-alpha (GRO-alpha): roles in atherosclerosis, angiogenesis and other inflammatory conditions. *Med. Sci. Monit.* **13**, RA87–RA90

33. Griffin, C. A., Apponi, L. H., Long, K. K., and Pavlath, G. K. (2010) Chemokine expression and control of muscle cell migration during myogenesis. *J. Cell Sci.* **123**, 3052–3060

34. Brzoska, E., Kowalewska, M., Markowska-Zagrajek, A., Kowalski, K., Archacka, K., Zimowska, M., Grabowska, I., Czerwińska, A. M., Czarnecka-Góra, M., Stremińska, W., Jańczyk-Ilach, K., and Ciemerych, M. A. (2012) Sdf-1 (CXCL12) improves skeletal muscle regeneration via the mobilisation of Cxcr4 and CD34 expressing cells. *Biol. Cell* **104**, 722–737

35. Issa, R., Xie, S., Lee, K. Y., Stanbridge, R. D., Bhavsar, P., Sukkar, M. B., and Chung, K. F. (2006) GRO-alpha regulation in airway smooth muscle by IL-1beta and TNF-alpha: role of NF-kappaB and MAP kinases. *Am. J. Physiol. Lung Cell. Mol. Physiol.* **291**, L66–L74

36. Lo, H. M., Shieh, J. M., Chen, C. L., Tsou, C. J., and Wu, W. B. (2013) Vascular endothelial growth factor induces CXCL1 chemokine release via JNK and PI-3K-dependent pathways in human lung carcinoma epithelial cells. *Int. J. Mol. Sci.* **14**, 10090–10106

37. Lo, H. M., Lai, T. H., Li, C. H., and Wu, W. B. (2014) TNF-α induces CXCL1 chemokine expression and release in human vascular endothelial cells in vitro via two distinct signaling pathways. *Acta Pharmacol. Sin.* **35**, 339–350

38. Peng, H., Wu, Y., Duan, Z., Ciborowski, P., and Zheng, J. C. (2012) Proteolytic processing of SDF-1α by matrix metalloproteinase-2 impairs CXCR4 signaling and reduces neural progenitor cell migration. *Protein Cell* **3**, 875–882

39. Starr, A. E., Dufour, A., Maier, J., and Overall, C. M. (2012) Biochemical analysis of matrix metalloproteinase activation of chemokines CCL15 and CCL23 and increased glycosaminoglycan binding of CCL16. *J. Biol. Chem.* **287**, 5848–5860

40. Dean, R. A., Cox, J. H., Bellac, C. L., Doucet, A., Starr, A. E., and Overall, C. M. (2008) Macrophage-specific metalloelastase (MMP-12) truncates and inactivates ELR+ CXC chemokines and generates CCL2, -7, -8, and -13 antagonists: potential role of the macrophage in terminating polymorphonuclear leukocyte influx. *Blood* **112**, 3455–3464

41. Hatfield, K. J., Reikvam, H., and Bruserud, Ø. (2010) The crosstalk between the matrix metalloprotease system and the chemokine network in acute myeloid leukemia. *Curr. Med. Chem.* **17**, 4448–4461

42. Ohtake, Y., Tojo, H., and Seiki, M. (2006) Multifunctional roles of MT1-MMP in myofiber formation and morphostatic maintenance of skeletal muscle. *J. Cell Sci.* **119**, 3822–3832

43. Bedair, H., Liu, T. T., Kaar, J. L., Badlani, S., Russell, A. J., Li, Y., and Huard, J. (2007) Matrix metalloproteinase-1 therapy improves muscle healing. *J. Appl. Physiol.* **102**, 2338–2345